

Trigeminal Nerve Neurofibroma Presenting as Facial Swelling in Two 3-year-olds

Jonathan Ferro, MS¹, Stephen Sozio, DO, MBS^{1*}, Lilun Li, MD², Sudipta Roychowdhury, MD¹ and Sri Hari Sundararajan, MD¹

¹Department of Radiology, Rutgers Robert Wood Johnson Medical School, New Brunswick, NJ, USA

²Department of Otolaryngology, Rutgers Robert Wood Johnson Medical School, New Brunswick, NJ, USA

*Correspondence to:

Stephen Sozio
Department of Radiology, Rutgers Robert Wood Johnson Medical School,
New Brunswick, NJ, USA.
E-mail: sjs335@rwjms.rutgers.edu

Received: October 03, 2023

Accepted: November 01, 2023

Published: November 06, 2023

Citation: Ferro J, Sozio S, Li L, Roychowdhury S, Sundararajan SH. 2023. Trigeminal Nerve Neurofibroma Presenting as Facial Swelling in Two 3-year-olds. *J Med Imaging Case Rep* 7(2) 55-60.

Copyright: © 2023 Ferro et al. This is an Open Access article distributed under the terms of the Creative Commons Attribution 4.0 International License (CCBY) (<http://creativecommons.org/licenses/by/4.0/>) which permits commercial use, including reproduction, adaptation, and distribution of the article provided the original author and source are credited.

Published by United Scientific Group

Abstract

Background: The trigeminal nerve (cranial nerve V) serves a pivotal role in sensory and motor functions within the head and neck. Although trigeminal schwannomas are the most common subtype of cranial nerve tumoral pathology, other peripheral nerve-based tumors can also be encountered, with neurofibroma remaining one of the top considerations in the differential diagnosis of a trigeminal nerve-based lesion.

Case presentation: Two unrelated 3-year-old females, one of whom carried a previously established diagnosis of neurofibromatosis type 1 (NF1), presented to the Emergency department (ED) with similar presentations of facial swelling. Each patient underwent imaging using a combination of ultrasound, Computed tomography (CT), and/or Magnetic resonance imaging (MRI), which revealed underlying tumors as the source of their facial swelling. Based on the tumor's imaging characteristics, both masses were diagnosed as trigeminal nerve neurofibromas.

Discussion: Nerve-based tumors can be identified by associating their location with an underlying nerve, which can be determined by examining CT or MRI imaging for remodeling or expansion of bony landmarks associated with the affected nerve(s). While schwannoma and neurofibroma share many imaging characteristics, and thus can be challenging to differentiate on imaging, the shape of the mass and relationship with its underlying nerve aid in narrowing the differential diagnosis.

Conclusion: It remains imperative to consider neurofibroma in the differential diagnosis of a nerve-based tumor. Early diagnosis and intervention can profoundly impact the treatment course and prognosis for patients suffering nerve-based tumors.

Keywords

Trigeminal nerve, Neurofibroma, Neurofibromatosis, Magnetic resonance imaging

Introduction

The cranial nerves, consisting of 12 distinct pairs, are responsible for numerous specialized functions vital to human physiology. Among these, the trigeminal nerve, or cranial nerve V, is a mixed nerve carrying both sensory and motor neurons which enable sensation to the head and neck, and movement of muscles of mastication [1]. Understanding the intricate function, anatomical distribution, and branches of the trigeminal nerve is essential, given the potential involvement of various pathologies affecting its distinct segments.

Trigeminal nerve tumors are exceedingly rare, accounting for only 0.07 - 0.3% of all intracranial tumors and they have the potential to affect any segment or branch of the trigeminal nerve [2]. Among the various types, trigeminal schwannomas are the most encountered tumors associated with the trigeminal nerve, typically presenting initially with trigeminal nerve dysfunction [2]. Although these tumors can arise at any portion along the trigeminal nerve, the cisternal segment, trigeminal/Gasserian ganglion in Meckel's cave, and the three peripheral nerve branches (V1, V2, V3) are the most frequently involved sites [2].

Given the rarity of trigeminal nerve tumors, determining their most prevalent location on the nerve can be challenging. A study conducted by Goel et al. analyzed 28 cases of trigeminal neurinomas (schwannomas) from 1989 to 2009. The study revealed that among the discussed cases, 4 neurinomas involved the ophthalmic division, 5 involved the maxillary division and 13 involved the mandibular division. However, it is important to note that the location of 6 tumors could not be determined due to extracranial involvement [3].

These two case reports present the clinical course of two 3-year-old female patients who presented to the hospital with left-sided facial swelling. The first case reports progressive nature of the swelling combined with the absence of oral complications after a tooth extraction, prompting further investigation. Through a multidisciplinary approach involving radiology, ENT, genetics, and pathology, a diagnosis of NF1 was made. The second case involves another 3-year-old female who recently immigrated from Guatemala with a known diagnosis of NF1. She presented to the ED with a progressively enlarging right facial mass. This resulted in further investigation with consults and imaging which revealed a neurofibroma within the trigeminal nerve distribution. These case reports highlight the difficulties of diagnosing neurofibromatosis and neurofibromas with an atypical presentation.

Review of Relevant Trigeminal Nerve Anatomy

The trigeminal nerve originates at the annular protuberance adjacent to the cerebellar peduncles and emerges from the pons through two nerve roots – a larger sensory root and a smaller motor root [4]. Traveling anteriorly, laterally, and cephalad from the annular protuberance, the two roots traverse toward the trigeminal cave, also known as the trigeminal cave of Meckel, or Meckel's cave [4]. Situated within the middle cranial fossa between the prepontine cistern and cavernous sinus, the trigeminal cave is composed of two layers of dura mater, serving as a vital anatomical landmark housing the sensory ganglion and trigeminal nerve roots [4]. The precavernous segment of the internal carotid artery courses inferomedially to the cave [5]. Notably, this cave assumes significance as a conduit for the spread of certain neoplasms [5]. The small size of the cave raises suspicion for developmental hypoplasia of the ipsilateral trigeminal nerve and subsequent neuropathy or myalgia [6]. Within the trigeminal cave, the trigeminal nerve branches into three distinct divisions: ophthalmic (V1), maxillary (V2), and mandibular (V3) nerves [1].

The ophthalmic branch represents the smallest division of the trigeminal nerve, exclusively responsible for sensory function. It primarily facilitates sensations pertaining to the scalp, eye, nose, and forehead [1]. Originating from the anteromedial portion of the trigeminal ganglion, the ophthalmic branch follows an oblique and superomedial course towards the superior orbital fissure [4]. It is important to understand the relationship the ophthalmic branch has with other important anatomical structures. Notably, the ophthalmic nerve passes beneath the trochlear nerve and intersects with parts of the carotid plexus [4].

The maxillary nerve originates from the central portion of the trigeminal ganglion, representing a sensory division of the trigeminal nerve. Exiting the skull through the foramen rotundum, it transverses the pterygopalatine fossa, which lies between the maxilla, sphenoid, and palatine bones [4, 7]. Subsequently, the maxillary nerve enters the inferior orbital fissure, crossing the infra-orbital groove to emerge on the facial region through the infra-orbital foramen [4]. Sensory innervation provided by the maxillary nerve encompasses derivatives of the first pharyngeal arch, primarily involving the middle third of the face [8]. Furthermore, the maxillary nerve also carries postganglionic fibers from the pterygopalatine ganglion, which innervates the lacrimal gland and mucous glands of the nose [8].

The mandibular branch of the trigeminal nerve serves particular importance due to its large size and composition of mixed neurons. The mandibular branch of the trigeminal nerve emerges from the lateral aspect of the trigeminal ganglion, consisting of both sensory and motor neurons [4]. Anatomically, the anterior portion of the mandibular nerve predominantly comprises motor neurons, while the posterior portion is primarily composed of sensory neurons [9]. A dural sheath envelops both the sensory and motor nerve roots as they traverse the foramen ovale [4]. Upon exiting the foramen ovale, the combined nerves diverge [4]. The sensory component of the mandibular nerve provides innervation to the gums, mandibular teeth, mucosa of the anterior tongue, floor of the oral cavity, skin in the temporal region of the head, lower lip, and external acoustic meatus [9]. Conversely, the anterior portion of the mandibular branch primarily innervates the muscles of mastication, including the medial and lateral pterygoids, temporalis, and masseter [9].

Case Presentation

Case 1

A 3-year-old female with no significant medical history presented to the hospital with left-sided facial swelling that had been progressively worsening over two months. The onset of swelling reportedly occurred following a tooth extraction and she was treated with antibiotics for presumed post-operative infection without resolution of swelling. Physical examination revealed a mobile, fluctuant left-sided facial mass measuring approximately 3 cm in diameter, without overlying tenderness or skin changes. Laboratory results, including blood cell count, amylase, and basic metabolic panel, were within normal limits. She was admitted for inpatient evaluation and multidisciplinary consultations.

A bedside ultrasound, as illustrated in **figure 1**, initially revealed a complex structure suggestive of the parotid gland, which exhibited cobblestoning but without evidence of a discrete fluid collection. A subsequent CT scan of the neck with IV contrast was performed, as illustrated in **figure 2**, which demonstrates a soft tissue mass within the left pterygopalatine fossa which extends laterally to the into the infratemporal fossa/masticator space through the pterygomaxillary fissure. This mass results in bony remodeling of the adjacent bony structures, and results in asymmetric widening and remodeling of the left inferior orbital fissure, left foramen ovale, as well as the ipsilateral foramen rotundum, sphenopalatine foramen, and palatine canal. Additionally, an asymmetric soft tissue density containing internal fatty streaks is present superficial to the left masseter muscle.

On hospital day 4, an MRI of the neck without and with IV contrast was performed for further characterization of this mass, as illustrated in **figure 3**. MRI revealed an irregularly shaped T1 hypointense, T2 hyperintense, homogeneously enhancing mass within the left infratemporal fossa which corresponds to the left pterygopalatine fossa mass visualized on CT. Mild deformity of the posterior aspect of the left maxillary sinus and left orbit is present due to underlying mass effect. The mass courses through the left pterygopalatine fossa, foramen ovale, and Meckel's cave, following the distribution of the V3 branch of the trigeminal nerve. Additionally, linear enhancement projected inferiorly from the mass to the subcutaneous mass within the left cheek, confirming that the mass follows the course of V3.

A biopsy of the buccal portion of the mass confirmed an abnormal proliferation of peripheral nerves with myxoid change within fibroadipose tissue, with histopathological features compatible with neurofibroma, or nerve sheath myxoma. The patient subsequently underwent genetic testing using the NF comprehensive panel through GeneDx, which revealed a likely pathogenic variant in the neurofibromatosis 2 gene

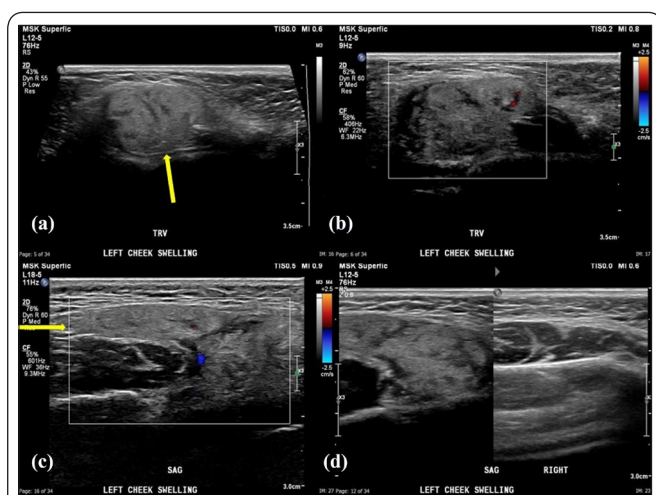


Figure 1: Bedside ultrasound of the left cheek, focused on the location of swelling. (a) Transverse imaging reveals a complex, heterogeneous structure adjacent to the left parotid gland which exhibits cobblestoning (yellow arrow). (b) Doppler imaging in the transverse plane of this complex structure reveals no significant internal vascularity. (c) Redemonstration of the complex, heterogeneous structure in the sagittal plane (yellow arrow). (d) Comparison of the left and right cheeks in the area of clinical concern confirms the left-sided asymmetry.

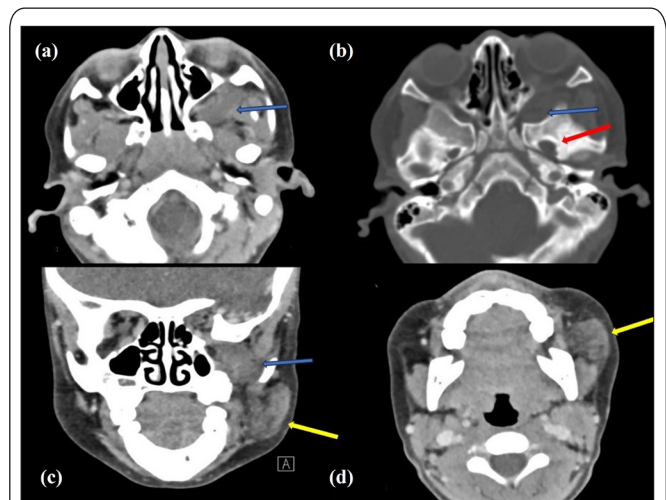


Figure 2: Contrast-enhanced CT facial bones. (a) Asymmetric soft tissue mass is present within the left pterygopalatine fossa (blue arrow), which extends laterally into the infratemporal fossa/masticator space through the pterygomaxillary fissure. (b) Axial imaging optimized for visualization of bony structures show the left pterygopalatine fossa mass asymmetrically widening the left inferior orbital fissure (blue arrow), left foramen ovale (red arrow), with corresponding bony remodeling. (c) Coronal image reveals the left pterygopalatine fossa soft tissue mass expanding the left inferior orbital fissure (blue arrow), in addition to an asymmetric soft tissue density anterior to the left parotid gland, superficial to and extending slightly anterior to the left masseter muscle (yellow arrow). This soft tissue density projects superiorly toward the left pterygopalatine fossa mass, and thus was suspected to be a contiguous extension. (d) Axial image confirms the asymmetric soft tissue density immediately anterior to the left parotid gland.

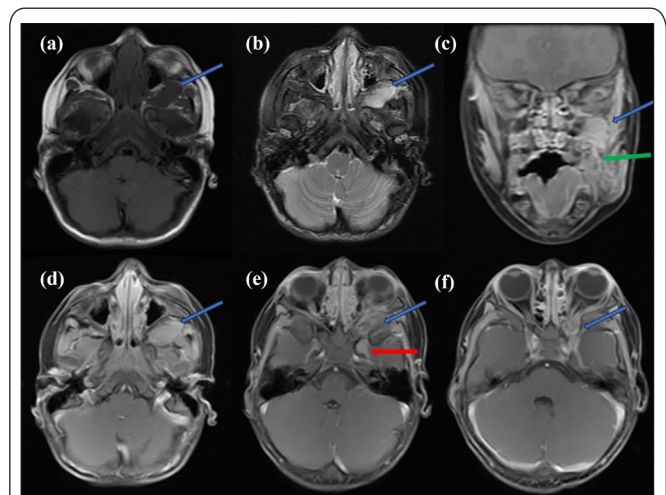


Figure 3: MRI of the facial bones. (a) Pre-contrast axial T1 imaging reveals a T1 hypointense mass within the left infratemporal fossa (blue arrow). (b) Pre-contrast axial fat-suppressed T2 sequence illustrates this left infratemporal fossa mass to be homogeneously T2 hyperintense. (c) Contrast-enhanced coronal T1 sequence demonstrates homogenous, avid enhancement of the left infratemporal fossa mass, which expands the ipsilateral inferior orbital fissure. Linear enhancement extends inferiorly from the mass to connect to the ipsilateral cheek soft tissue mass, which sits immediately adjacent to the mandible (green arrow). (d, e, f) Contrast-enhanced axial T1 imaging confirms homogenous, avid enhancement of the left infratemporal mass (blue arrow), which extends into Meckel's cave (red arrow).

(c.367 A > T). This finding, combined with the imaging findings, fulfilled the diagnostic criteria for NF1. As the patient had no localized pain, motor deficits, or ophthalmologic deficits, immediate open surgical resection was deferred due to

associated morbidity, in anticipation of a less-invasive endoscopic resection following maturation of her paranasal sinuses.

Case 2

A 3-year-old, ex-full term twin female with a medical history of NF1 who presented to the ED with several months of progressively enlarging facial mass, congestion, upper respiratory infection symptoms. Her enlarging facial mass had been biopsied approximately two years prior in her native country and diagnosed as neurofibroma. She had recently immigrated to the United States with her family, seeking a better level of care for her genetic condition, after being diagnosed in her native country of Guatemala and told that there were no treatment options available to her. As a result of her enlarging facial mass, she experienced trouble chewing, difficulty speaking, and an inability to fully close her right eye. Her physical examination revealed marked swelling on the right side of her face, limited tongue mobility, and right sided esotropia due to the large underlying mass. Additionally, hyperpigmented macules were present throughout her trunk and lower extremities bilaterally. A contrast-enhanced CT of her head and facial bones was performed, as illustrated in figure 4. Initial laboratory testing was positive for rhinovirus, and she was ultimately admitted to the hospital for further management.

During her hospital stay, she underwent multiple specialist consultations, and underwent a contrast-enhanced MRI of the Brain, Orbits, and Soft Tissue Neck, as illustrated in figure 5. A further MRI of the spine was initially proposed, but not performed, due to the extended time under sedation for the head and neck examinations. Given the extent of her disease and associated morbidity, the patient was not a surgical candidate for resection. Prior to discharge, she was recommended by the oncology team to be initiated on selumetinib, an oral selective MEK 1 and 2 inhibitor that was FDA-approved in 2020 for the treatment of symptomatic, inoperable plexiform neurofibromas in pediatric patients aged 2 years or older with NF1 [10, 11].

Results and Discussion

Neurofibromas are peripheral nerve sheath tumors which arise due to mutation in the NF1 gene, and histologically consist of Schwann cells, fibroblasts, perineural cells, and mast cells [12]. When diagnosing neurofibromas, familiarity with the characteristic imaging features on ultrasound, CT and MRI remains pivotal. On ultrasound, neurofibroma appears as a well-defined oval hypoechoic mass which is continuous with peripheral nerves, as reflected in the soft tissue ultrasound in case 1, although delineation of continuity with a peripheral nerve was not possible [13]. CT imaging of neurofibromas will reveal a hypoattenuating soft-tissue mass, which exhibits minimal or no contrast enhancement [13]. Again, given that neurofibroma is a nerve sheath tumor, the tumor will be located along the course of a nerve, although delineation may not be directly apparent in the setting of large masses. In times when this is not directly apparent, one practice our group has adopted is the utilization of bone-reconstructed sequences to search for expansion or remodeling at bony landmarks associated with the nerve. As neurofibromas are comparatively slow-growing

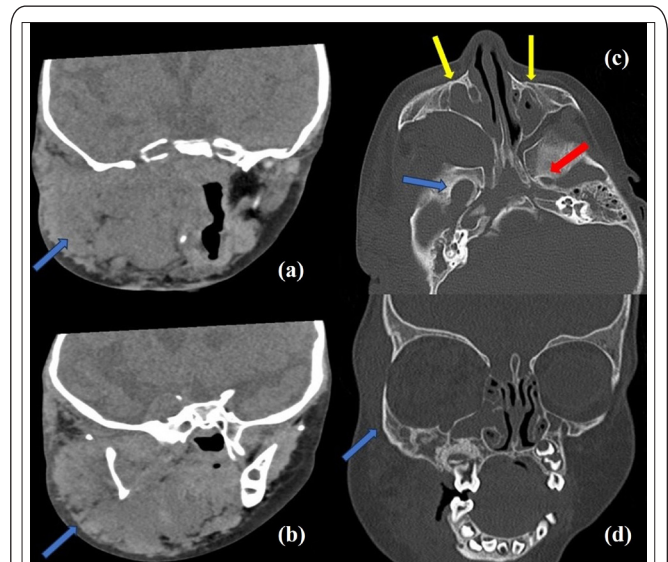


Figure 4: Contrast-enhanced CT of the head and facial bones, which demonstrates a broad, multiloculated, trans-spatial mass. (a) Soft tissue optimized coronal image demonstrating a large soft tissue mass expanding the right parotid, preauricular, and temporoparietal scalp soft tissues (blue arrow). (b) Additional soft tissue optimized coronal image slice reveals extension of this mass into the right masticator, submandibular, and sublingual spaces (blue arrow). (c) Bone-optimized axial slice illustrating asymmetric remodeling and enlargement of the right foramen ovale (blue arrow), when compared to that of the left side (red arrow). Diminutive-sized and predominately opacified maxillary sinuses are also demonstrated (yellow arrows). (d) Bone-optimized coronal imaging illustrates remodeling and outward expansion of the right sided facial bones, a consequence of the long-standing nature of the underlying mass. Circumferential remodeling and enlargement of the right orbit and zygomatic arch is illustrated by the blue arrow.

processes, chronic osseous expansion and remodeling occurs along the affected nerve at these key landmarks. This finding was present in both cases presented in this manuscript, as the direct association of tumor with the trigeminal nerve became grossly apparent through bony remodeling and expansion of the foramen ovale and was further supported in case 1 by remodeling of the inferior orbital fissure.

On MRI, neurofibromas exhibit T1 hypointense and T2 hyperintense signal, with avid post-contrast enhancement [13]. A characteristic “target sign,” defined as a T2 hyperintense peripheral rim and a hypointense central component, has been classically associated with neurofibroma, although it is important to note that this finding can be observed in other nerve sheath tumors [13]. Additionally, the presence of a fascicular sign also supports the diagnosis of a neurogenic lesion, which appears as multiple small ring-like foci with a peripheral hyperintense band [13]. In parallel to CT, bony landmarks along the course of any nerve(s) suspected to be involved should be assessed on every MRI examination, as bony expansion and remodeling supports the diagnosis of a nerve-based tumor. Again, it is imperative to note that the presence of bony remodeling along the course of a nerve, and/or the presence of either a target sign or a fascicular sign, solely support the premise that a tumor is nerve sheath-based and cannot reliably differentiate between different types of nerve sheath-based tumors. Of note, neither a target sign nor a fascicular sign was visualized in either patient’s examinations.

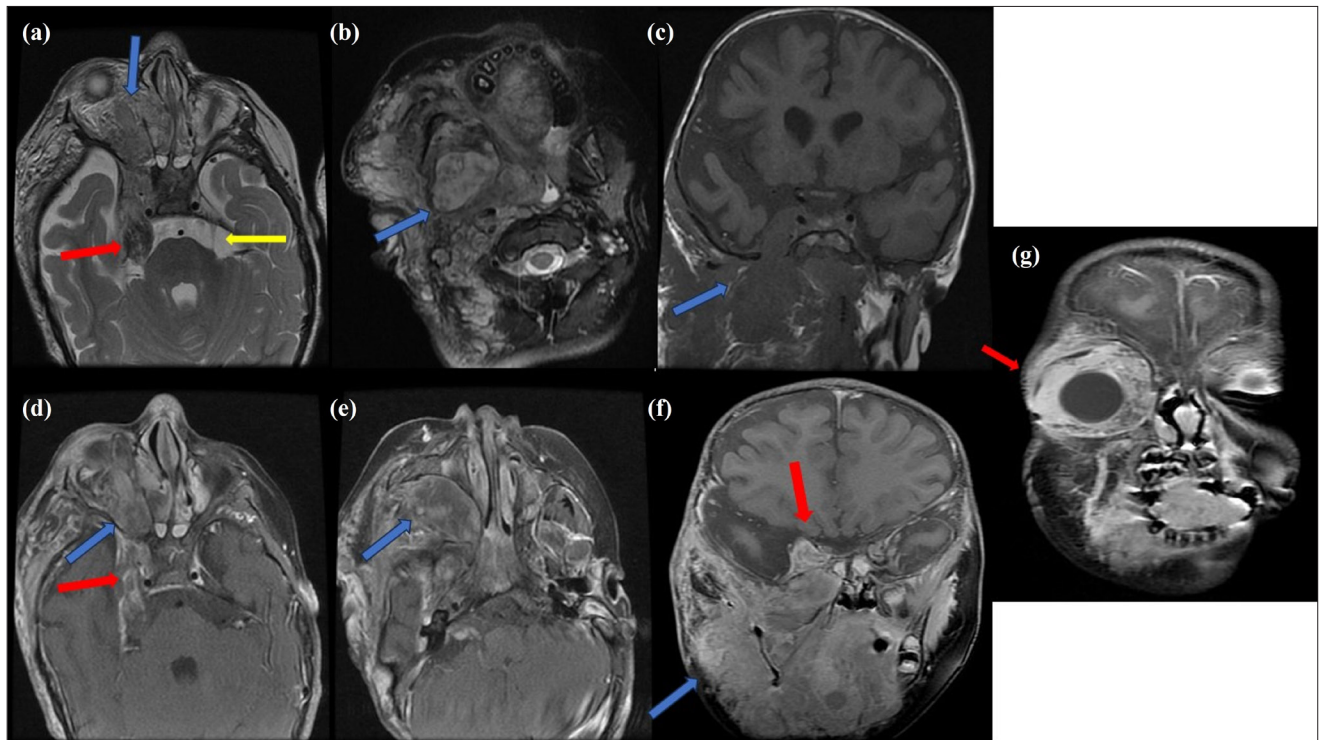


Figure 5: MRI of the brain, orbits, and soft tissue neck. (a) Axial T2 pre-contrast imaging reveals a large heterogenous plexiform mass extending along the course of the right trigeminal nerve, coursing through Meckel's cave (Red) and extending anteriorly through the pterygopalatine fossa to the right orbit, resulting in right-sided exophthalmos (blue arrow). A normal appearing left trigeminal nerve is illustrated by the yellow arrow, for comparison. (b) Axial T2 fat-suppressed pre-contrast sequence confirms the heterogenous plexiform mass to invade the right-sided muscles of mastication and parotid space (blue arrow). Cystic foci contained within the mass are suspected of necrosis. (c) Coronal T1 pre-contrast sequence confirms the mass to be predominately T1 hypointense and extends along the trigeminal nerve distribution (blue arrow). (d) Contrast-enhanced axial T1 fat suppressed imaging confirms the mass to exhibit heterogenous enhancement, again extending along the course of the trigeminal nerve through Meckel's cave (blue and red arrows). (e) Contrast-enhanced axial T1 fat suppressed slice, similar in location compared to the prior CT Head, demonstrates tracking of the mass along the right parapharyngeal region and the right-sided mastication muscle (blue arrow). (f) Contrast-enhanced coronal T1 imaging illustrates the mass to track along the right parapharyngeal region and the right-sided muscles of mastication, extending to expand the right sided cheek soft tissues. (g) Contrast-enhanced coronal T1 imaging illustrating right-sided exophthalmos as a result of the underlying mass (red arrow).

While the majority of neurofibroma cases are sporadic, others are associated with genetic conditions, most commonly NF1 or NF2 [12]. Neurofibromatosis is considered a group of disorders encompassing three distinct diseases: NF1, NF2, and schwannomatosis, with NF1 being the most prevalent [14]. NF1 is a disease of variable expressivity rooted in a mutation of the neurofibromin protein, a tumor suppressor gene, resulting in the development of multiple central and peripheral nerve tumors [14]. Central nerve tumors, frequently observed in NF1, include optic pathway glioma, astrocytoma's, and brain stem gliomas [15]. Optic pathway gliomas affect approximately 15 - 20% of individuals with NF1 and predominantly manifest in children younger than seven years old. On MRI, these tumors present as swollen optic nerves with avid post-contrast enhancement [15]. Brain stem gliomas, also categorized as pilocytic astrocytoma's, primarily affect older children (seven to eight years old), and can develop in any part of the brainstem, appearing on MRI with a characteristic 'cyst-within-a-nodule' appearance [15].

Recognizing neurofibromatosis in pediatric patients is essential for comprehensive assessment, effective management, and successful treatment of complex conditions. Specifically, NF1 typically manifests during infancy with a constellation of clinical features, including café-au-lait spots, sphenoid bone dysplasia, pseudoarthrosis, and plexiform neurofibromas [16].

During early childhood, NF1 may manifest with motor and speech delays, autism spectrum disorder, attention deficit disorder, and various learning difficulties [16].

As adolescences, the clinical picture of NF1 evolves to encompass axillar and inguinal freckles, Lisch nodules, scoliosis, the emergence of neurofibromas, and the development gliomas, with optic gliomas being the most prevalent among pediatric gliomas [16]. It is important to acknowledge the association between NF1 and chronic pain, which is supported by a study conducted by Kongkriangkai et al. [17], which demonstrated that that pain affected 55% of both pediatric and adult patients suffering NF1 within the cohort. Thus, in the appropriate clinical context, the presence of unexplained and/or chronic pain can increase suspicion for NF1 in the pediatric population.

Managing NF1, especially in children, presents unique challenges due to its systemic involvement. However, a promising avenue of treatment lies in gene therapy, offering the potential for a curative outcome by either replacing or substituting the defective genetic mutation with a functional form of neurofibromin [16]. Additional treatments utilizing RAS inhibitors are also under investigation, such as Sorafenib, which inhibits overactivation of the RAS oncogene as it serves a pivotal role in NF1 pathophysiology [16]. Beyond medication,

surgical interventions and radiation therapy have also been employed in cases of severe NF1, in which tumor debulking is required.

Understanding the radiographic distinctions between schwannoma and neurofibroma is crucial, as schwannoma is the most encountered peripheral nerve sheath tumor, including within cranial nerves, and frequently the top consideration in the imaging differential diagnosis [18]. Specific to cranial nerves, the vestibulocochlear nerve being the most commonly involved in a schwannoma, followed by the trigeminal and facial nerves as the second and third most common sites, respectively [18].

On CT imaging, schwannoma appears as a hypo-to-isointense mass and exhibits avid post-contrast enhancement, which may appear somewhat heterogeneous in larger tumors [18]. MRI is the most useful modality in differentiating schwannoma, where it appears T1 hypo-to-isointense, T2 heterogeneously hyperintense, and exhibit avid post-contrast enhancement, which also may appear heterogeneous in larger masses [18]. Aside from subtle differences in signal and contrast enhancement, schwannomas tend to displace their associated nerves, while neurofibromas appear to encase their associated nerves [18]. Furthermore, schwannomas may appear as more rounded masses, while neurofibromas are more fusiform in appearance [18, 19].

Conclusion

These case reports highlight the significance of considering a neurofibroma in the differential diagnosis when encountering patients with masses of unknown origin in the craniofacial compartments. It is crucial to recognize that neurofibromas can arise in various locations throughout the body and along any nerve, including along the cranial nerves. In supplement to imaging characteristics, nerve-based tumors can, in part, be distinguished by remodeling of bony landmarks associated with the affected nerve(s). Prompt and accurate diagnosis of a neurofibroma promotes effective multidisciplinary triage and management, which typically includes either continued observation, initiation of licensed medicinal therapy such as selumetinib, or surgical resection.

Acknowledgements

None.

Conflicts of Interest

None.

References

- Huff T, Weisbrod LJ, Daly DT. 2018. Neuroanatomy, Cranial Nerve 5 (Trigeminal). StatPearls.
- Agarwal A. 2015. Intracranial trigeminal schwannoma. *Neuroradiol J* 28(1): 35-41. <https://doi.org/10.15274/NRJ-2014-10117>
- Goel A, Shah A, Muzumdar D, Nadkarni T, Chagla A. 2010. Trigeminal neurinomas with extracranial extension: analysis of 28 surgically treated cases. *J Neurosurg* 113(5): 1079-1084. <https://doi.org/10.3171/2009.10.JNS091149>
- Barral JP, Croibier A. 2009. *Manual Therapy for the Cranial Nerves*. Elsevier, Edinburgh.
- Malhotra A, Tu L, Kalra VB, Wu X, Mian A, et al. 2018. Neuroimaging of Meckel's cave in normal and disease conditions. *Insights Imaging* 9: 499-510. <https://doi.org/10.1007/s13244-018-0604-7>
- Sundararajan S, Loevner LA, Mohan S. 2018. Mandibular myalgia and miniscule Meckel's caves. *J Otorhinolaryngol Relat Spec* 80(2): 103-107. <https://doi.org/10.1159/000489462>
- Aoun G, Zaarour I, Sokhn S, Nasseh I. 2015. Maxillary nerve block via the greater palatine canal: an old technique revisited. *J Int Soc Prev Community Dent* 5(5): 359. <https://doi.org/10.4103/2231-0762.165930>
- Shafique S, Das JM. 2019. *Anatomy, Head and Neck, Maxillary Nerve*. StatPearls.
- Somayaji SK, Acharya SR, Mohandas KG, Venkataramana V. 2012. Anatomy and clinical applications of the mandibular nerve. *Bratisl Lek Listy* 113(7): 431-440. https://doi.org/10.4149/bl_2012_097
- Gross AM, Wolters PL, Dombi E, Baldwin A, Whitcomb P, et al. 2020. Selumetinib in children with inoperable plexiform neurofibromas. *N Engl J Med* 382(15): 1430-1442. <https://doi.org/10.1056/NEJMoa1912735>
- Anderson MK, Johnson M, Thornburg L, Halford Z. 2022. A review of selumetinib in the treatment of neurofibromatosis type 1-related plexiform neurofibromas. *Ann Pharmacother* 56(6): 716-726. <https://doi.org/10.1177/10600280211046298>
- Messersmith L, Krauland K. 2019. *Neurofibroma*. StatPearls.
- Wang MX, Dillman JR, Guccione J, Habiba A, Maher M, et al. 2022. Neurofibromatosis from head to toe: what the radiologist needs to know. *Radiographics* 42(4): 1123-1144. <https://doi.org/10.1148/rg.210235>
- Cimino PJ, Gutmann DH. 2018. Neurofibromatosis type 1. *Handb Clin Neurol* 148: 799-811. <https://doi.org/10.1016/B978-0-444-64076-5.00051-X>
- Campian J, Gutmann DH. 2017. CNS tumors in neurofibromatosis. *J Clin Oncol* 35(21): 2378. <https://doi.org/10.1200/JCO.2016.71.7199>
- Sur ML, Armat I, Sur G, Pop DC, Samasca G, et al. 2022. Neurofibromatosis in children: actually and perspectives. *Children* 9(1): 40. <https://doi.org/10.3390/children9010040>
- Kongkriangkai AM, King C, Martin LJ, Wakefield E, Prada CE, et al. 2019. Substantial pain burden in frequency, intensity, interference and chronicity among children and adults with neurofibromatosis type 1. *Am J Med Genet A* 179(4): 602-607. <https://doi.org/10.1002/ajmg.a.61069>
- Skolnik AD, Loevner LA, Sampathu DM, Newman JG, Lee JY, et al. 2016. Cranial nerve schwannomas: diagnostic imaging approach. *Radiographics* 36(5): 1463-1477. <https://doi.org/10.1148/rg.2016150199>
- Armstrong AE, Belzberg AJ, Crawford JR, Hirbe AC, Wang ZJ. 2023. Treatment decisions and the use of MEK inhibitors for children with neurofibromatosis type 1-related plexiform neurofibromas. *BMC Cancer* 23(1): 1-12. <https://doi.org/10.1186/s12885-023-10996-y>